May 2001

First results on the running coupling in QCD with two massless flavours

ALPHA
Collaboration

Achim Bode[a], Roberto Frezzotti[b,c], Bernd Gehrmann[d],
Martin Hasenbusch[d], Jochen Heitger[e], Karl Jansen[f], Stefan Kurth[d],
Juri Rolf[d], Hubert Simma[g], Stefan Sint[c,h], Rainer Sommer[g],
Peter Weisz[i], Hartmut Wittig[j] and Ulli Wolff[d]

[a] CSIT, Tallahassee, USA
[b] Dipt. di Fisica, Univ. di Milano Bicocca, Milano, Italy
[c] CERN-TH, Geneva, Switzerland
[d] Institut für Physik, Humboldt Universität, Berlin, Germany
[e] Institut für Theor. Physik, Universität Münster, Münster, Germany
[f] NIC, Zeuthen, Germany
[g] DESY, Zeuthen, Germany
[h] Dipt. di Fisica, Univ. di Roma, Tor Vergata, Rome, Italy
[i] Max-Planck-Institut für Physik, München, Germany
[j] Dept. of Mathematical Sciences, Univ. of Liverpool, Liverpool, UK

Abstract We report on the non-perturbative computation of the running coupling of two-flavour QCD in the Schrödinger functional scheme. The corresponding Λ-parameter, which describes the coupling strength at high energy, is related to a low energy scale which still remains to be connected to a hadronic "experimentally" observable quantity. We find the *non-perturbative* evolution of the coupling important to eliminate a significant contribution to the total error in the estimated Λ-parameter.

Keywords: lattice QCD; dynamical fermions; running coupling; renormalization.

PACS: 11.15.Ha; 12.38.Gc; 12.38.Bx; 11.10.Gh; 11.10.Hi

1 Introduction

Under lattice regularization predictions of renormalized quantum field theories emerge as universal properties of critical points of models in the appropriate universality class. In this way the theory is defined independently of perturbation theory and may for instance be evaluated numerically. Predictive power resides in a surplus of relations between observables over free parameters in the model, and it becomes a well-defined question which part of these relations is amenable to approximation by renormalized perturbation theory. In QCD the standard expectation is that quantities associated with energies large compared to typical hadron masses can be perturbatively related to each other. If one is limited to this calculational framework, a small number of input parameters associated with large normalization energy μ, like the coupling $\alpha_s(\mu)$ and the quark masses for each flavour $\overline{m}_f(\mu)$, have to be determined from experiment and then lead to many successful predictions of perturbative QCD.

By lattice techniques it becomes possible to look beyond the perturbative horizon. Consequently a lot of activity goes and went into extracting information on the hadronic low energy sector. In particular the free parameters are determined in this case by inputting quantities like some hadron masses or F_π. Then the high energy sector can in principle be predicted by *evaluating* $\alpha_s(\mu)$ and the quark masses for $\mu \gg F_\pi$. Such calculations relating different orders of magnitude of physical scales represent a formidable numerical problem. Beside the dissimilar physical scales, infrared and ultraviolet cutoffs have to be extrapolated to their respective limits. A number of such direct approaches have nevertheless been tried, and some have found their entry into the particle data table [1–4] as one of the most accurate determinations of $\alpha(M_Z)$. In view of the very limited parameter range accessible to simulation we find it difficult to be confident about the systematic errors of these determinations. A computation requiring more steps but also offering much more control of systematic errors becomes feasible by the recursive finite size method using the Schrödinger functional. This technique has been developed by our collaboration over the last years and is reviewed in [5] and [6].

In this publication we present first numerical results toward the extension of the method from the zero flavour (quenched) approximation to QCD with two light flavours which are taken massless. Sect. 2 summarizes the most essential results of our previous work in the present context. In sect. 3 the computational strategy for the Λ-parameter characterizing the coupling at large energy is outlined, followed by numerical results in sect. 4 and some conclusions.

1

2 Schrödinger functional setup

To connect hadronic and perturbative scales in QCD an intermediate renormalization scheme has been devised where the finite system size L is used as a renormalization scale. More precisely, we consider the Schrödinger functional given by the partition function of QCD on a cylinder of size $T \times L^3$ in euclidean space

$$e^{-\Gamma} = \int_{T \times L^3} D[U, \psi, \bar{\psi}] \, e^{-S} . \qquad (2.1)$$

In the lattice regularized form we integrate over SU(3) gauge fields U with the Wilson action and two flavours of $O(a)$ improved Wilson quarks $\psi, \bar{\psi}$. Boundary conditions in the spatial directions of length L are periodic [7] for U and periodic up to a global phase [8] $\theta = \pi/5$ for $\psi, \bar{\psi}$. In Euclidean time Dirichlet boundary conditions are imposed at $x_0 = 0, T$ by fixing spatial links to diagonal SU(3) matrices that are precisely specified in terms of L and two angles η and ν (point 'A' in [9]), and we also take $T = L$. The quark fields on the boundary surfaces [10] are given by Grassmann values $\rho, \bar{\rho}$ and $\rho', \bar{\rho}'$, which are used as sources that are set to zero after differentiation.

To achieve the convergence to the continuum limit at a rate proportional to the squared lattice spacing a^2 a number of irrelevant operators have to be tuned. The coefficient c_{SW} of the clover term [11] is set to the non-perturbative values quoted in parameterized form in [12]. In the Schrödinger functional at vanishing quark mass, that we consider here, the coefficients c_t and $\tilde{c}_t$ of two additional boundary counter terms [10] have to be adjusted. Here we have to content ourselves with perturbative estimates at one and two-loop accuracy [13,14].

Since for Wilson fermions chiral symmetry only emerges in the continuum limit, the bare mass parameter is additively renormalized. For this reason we trade it for a quark mass defined by the PCAC relation evaluated using suitable states [17]. Let $f_A(x_0)$ and $f_P(x_0)$ be the matrix elements of the axial current and the pseudoscalar density defined in (2.1) and (2.2) of [17] with the gluonic boundary fields assuming the values quoted above. We form the ratio

$$m(x_0) = \frac{\frac{1}{2}(\partial_0 + \partial_0^*) f_A(x_0) + c_A a \partial_0 \partial_0^* f_P(x_0)}{2 f_P(x_0)} \qquad (2.2)$$

with forward (backward) derivative ∂_0 (∂_0^*). For the current improvement coefficient c_A its one-loop value [13] is taken. We now define the bare current mass

$$m_1 = \begin{cases} m(T/2) & \text{for even } T/a \\ [m((T-a)/2) + m((T+a)/2)]/2 & \text{for odd } T/a. \end{cases} \qquad (2.3)$$

An alternative definition m_2 just differs by averaging $m(x_0)$ and $m'(x_0)$, where the latter is defined [17] with the sources $\rho', \bar{\rho}'$ at the $x_0 = T$ boundary leading to f_A', f_P'. These masses are expected to differ at $\mathrm{O}(a^2)$. With either of them vanishing, the chirally symmetric continuum limit may be approached.

The coupling $\bar{g}^2$ and the additional universal dimensionless observable $\bar{v}$ are related to the Schrödinger functional by

$$\frac{\partial \Gamma}{\partial \eta} = k \left\{ \frac{1}{\bar{g}^2(L)} - \nu \bar{v}(L) \right\}, \tag{2.4}$$

where k is a known [9] normalization fixed by demanding $\bar{g}^2 = g_0^2 + \mathrm{O}(g_0^4)$ with the bare coupling g_0.

3   Computational strategy for the Λ-parameter

Our method to extract Λ, which characterizes the behaviour of $\bar{g}^2$ at asymptotically large energy, follows the strategy used in [18]. By continuum extrapolation we construct the non-perturbative step scaling function (SSF)

$$\sigma(u) = \bar{g}^2(2L)|_{\bar{g}^2(L)=u, m_1=0} \tag{3.1}$$

for a number of u-values such that by interpolation we control it over the range that will be needed. Then a value $u_{\max}$ is selected (initially by guesswork) such that the associated scale $L_{\max}$ where $\bar{g}^2(L_{\max}) = u_{\max}$ is in the hadronic range. By recursively solving n times

$$\sigma(\bar{g}^2(L/2)) = \bar{g}^2(L) \tag{3.2}$$

starting with $L = L_{\max}$ we obtain values for $\bar{g}^2(2^{-n}L_{\max})$. Finally, for sufficiently large n, this coupling is perturbative and we use

$$\begin{aligned}
\Lambda L_{\max} &= 2^n (b_0 \bar{g}^2)^{-b_1/2b_0^2} \exp\left\{ -\frac{1}{2b_0\bar{g}^2} \right\} \\
&\quad \times \exp\left\{ -\int_0^{\bar{g}} dx \left[\frac{1}{\beta(x)} + \frac{1}{b_0 x^3} - \frac{b_1}{b_0^2 x} \right] \right\}
\end{aligned} \tag{3.3}$$

to derive Λ in terms of $L_{\max}$. Here the three-loop β-function[1] for the SF-scheme with two flavours [14] is used and b_0, b_1 are its universal coefficients. On the right-hand side $\bar{g}^2$ is understood to be inserted at the scale $2^{-n}L_{\max}$.

---

[1] We now use $b_2 = 0.06/(4\pi)^3$ given in the second erratum to [14] which has become necessary due to the revision of [15] in May 2001. Since our analysis depends on these results, an independent check seems desirable. It will be partially supplied in the near future [16].

The admissibility and accuracy of renormalized perturbation theory can be probed by checking the stability of the result when varying n.

In a later series of simulations we shall have to relate L_{max} to a truly physical scale, for instance by computing $L_{\mathrm{max}}F_\pi$. The guess for u_{max} will be confirmed then, if a number of order one is found, i. e. the multiple scale problem is avoided. The relation between Λ, which corresponds to the SF-scheme, and the $\overline{\mathrm{MS}}$-scheme is given by [8,14]

$$\Lambda_{\overline{\mathrm{MS}}} = 2.382035(3)\,\Lambda. \tag{3.4}$$

4 Numerical results

The continuum SSF is given by the limit

$$\sigma(u) = \lim_{a/L \to 0} \Sigma(u, a/L), \tag{4.1}$$

where Σ is defined like σ in eq. (3.1) but interpreted at finite resolution a/L. Since PCAC becomes an operator relation in the continuum limit only, we adopt the convention to always tune $m_1(L/a)$ to zero on the small lattice. The corresponding value $m_1(2L/a)$ measured at resolution $a/2L$ is expected to differ by $\mathrm{O}(a^2)$ from $m_1(L/a)$. In the same way we expect $m_1(L/a) - m_2(L/a) = \mathrm{O}(a^2)$ for our alternative definition m_2 of the bare current quark mass. We tested these expectations on our data and compared with one-loop perturbation theory in Fig. 1 for several couplings. Where available we include together with our present $N_{\mathrm{f}} = 2$ data also quenched and bermion [19] ($N_{\mathrm{f}} = -2$) results. We conclude that lattice artefacts behave non-pathologically and similar to perturbative expectations. For the accessible range of resolutions they happen to be dominated by terms of higher order than the expected a^2-contributions.

Another place to study the approach to universal continuum behaviour is the relation between $\bar{v}$ and $\bar{g}$ defined in (2.4),

$$\bar{v} = \omega(\bar{g}^2) = \lim_{a/L \to 0} \Omega(\bar{g}^2, a/L). \tag{4.2}$$

In perturbation theory Ω is known to two-loop order,

$$\Omega(u, a/L) = (v_1 + v_2 u)\left[1 + \epsilon_1(a/L) + \epsilon_2(a/L)u\right] + \mathrm{O}(u^2), \tag{4.3}$$

and ϵ_1, ϵ_2 encode the perturbative artefacts. In Fig. 2 data for two different values of the coupling are plotted. The square symbols refer to the improved
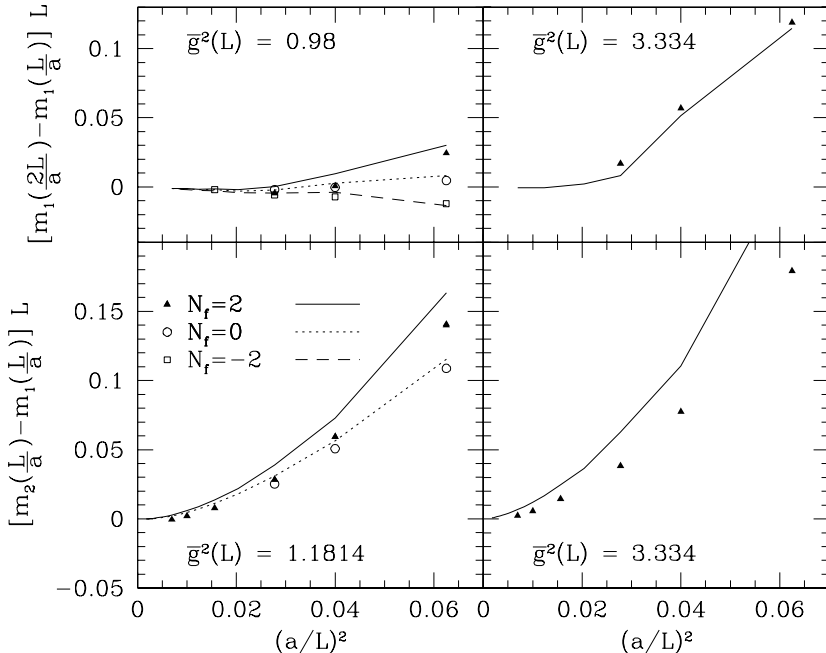
Figure 1: Lattice artefacts of PCAC masses. Perturbative results for integer L/a are connected by lines.

observable, where the Monte Carlo results have been divided by the perturbative lattice artefacts $1 + \epsilon_1(a/L) + \epsilon_2(a/L)u$ as first discussed in [20]. We conclude that a much smoother continuum limit is achieved in this way.

At present, due to limitations of computing power, we have results with sufficient statistics only for $\bar{g}^2$ on lattices with $L/a \leq 12$. The resulting values of Σ are collected in table 1. The algorithmic aspects of these simulations have been presented in [21].

To estimate a continuum value for σ from lattices with $L/a = 4, 5, 6$ (together with the lattices at the doubled lengths) we adopt the following procedure. First we perturbatively correct the data with a factor analogous to the one in eq. (4.3)

$$\Sigma(u, a/L) \rightarrow \Sigma^{(2)}(u, a/L) = \frac{\Sigma(u, a/L)}{1 + \delta_1(a/L)u + \delta_2(a/L)u^2} \qquad (4.4)$$

with the series for the artefacts known up to two-loop order. They depend, of course, on the details of the action chosen. As the two-loop boundary improvement coefficient $c_t(g_0)$ became available only during our simulations
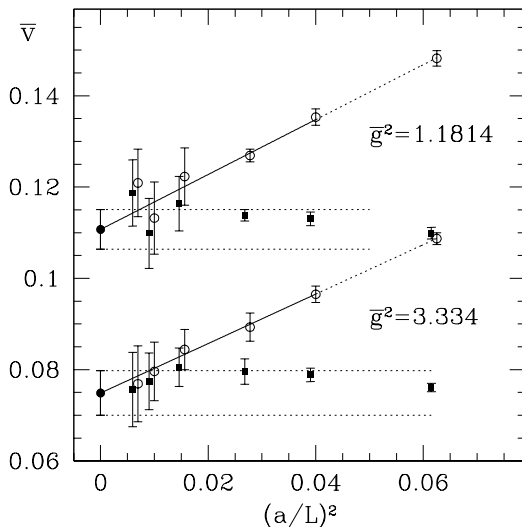
5

Figure 2: Circular symbols are data for $\bar{v}$ including a continuum extrapolation. Square symbols have perturbative lattice artefacts cancelled.

they were partly carried out with its one-loop value (left part of table 1) and only later with the two-loop value. Hence two different sets of δ_2 had to be used in (4.4). We found the values of $\Sigma^{(2)}(u, a/L)$ for $L/a = 5, 6$ constant within errors and fitted them to a constant (i. e. just combined them) as our present continuum estimates. They are found in table 2 together with $\Sigma^{(2)}$ at resolution $L/a = 4$ for the estimation of systematic errors (see below). In Fig. 3 the analogous procedure can be judged in the quenched case, where many more data are available. The averages of the points at $L/a = 5, 6$ in each series lead to the dotted lines and are to be compared with the full extrapolation (points at $a/L = 0$).

We interpolate the values of table 2 by fitting $\sigma(u)$ to a sixth order polynomial with the first three coefficients constrained to their perturbative values. The resulting SSF is shown in Fig. 4. It differs from the quenched SSF by an amount predicted well by perturbation theory for weak coupling. For values above about 2.5 the three-loop term contributes significantly to the β-function but actually enhances the growing gap between Monte Carlo results and perturbation theory.

The fitted form for σ is employed to estimate ΛL_{max} in the way described in sect. 2 starting from $u_{\mathrm{max}} = 3.3$ and from $u_{\mathrm{max}} = 5$. Statistical errors are obtained by propagating the errors of the primary Monte Carlo data through the whole analysis, and the inclusion of another parameter in the interpolating

L/a	u	Σ	u	Σ
4	0.9793(7)	1.0643(34)	1.5031(12)	1.720(5)
5	0.9793(6)	1.0721(39)	1.5033(26)	1.737(10)
6	0.9793(11)	1.0802(44)	1.5031(30)	1.730(12)
4	1.1814(5)	1.3154(55)	2.0142(24)	2.481(17)
5	1.1807(12)	1.3287(59)	2.0142(44)	2.438(19)
6	1.1814(15)	1.3253(67)	2.0146(56)	2.508(26)
4	1.5031(10)	1.731(6)	2.4792(34)	3.251(28)
5	1.5031(20)	1.758(11)	2.4792(73)	3.336(50)
6	1.5031(25)	1.745(12)	2.4792(82)	3.156(55)
4	1.7319(11)	2.058(7)	3.334(11)	5.298(85)
5	1.7333(32)	2.086(21)	3.334(15)	5.41(12)
6	1.7319(34)	2.058(20)	3.326(20)	5.68(13)

Table 1: Data for the lattice step scaling function $\Sigma(u, a/L)$. For the left part $c_{\mathrm{t}}(g_0)$ was set to its one-loop value, whereas the two rightmost columns have been obtained with the two-loop result [14].

u	$\sigma(u)$	$\Sigma^{(2)}(u, 1/4)$
0.9793	1.0768(30)	1.0686(35)
1.1814	1.3277(46)	1.3199(55)
1.5031	1.7489(85)	1.7332(60)
1.7319	2.063(15)	2.0562(72)
1.5031	1.750(8)	1.7477(56)
2.0142	2.494(16)	2.535(18)
2.4792	3.304(38)	3.338(28)
3.3340	5.65(10)	5.491(90)

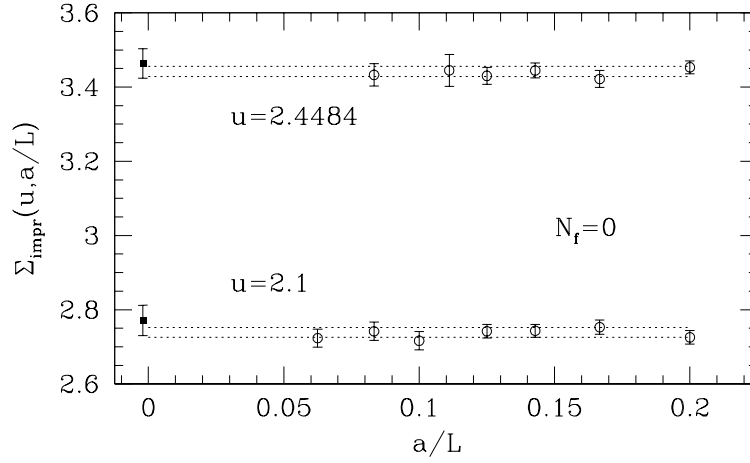Table 2: Numerical results for $\sigma(u)$.

Figure 3: Quenched results for $\Sigma^{(2)}$ to illustrate our extrapolation procedure. Data are mostly from the literature [9,16] apart from the two finest resolutions at $u = 2.1$ which were obtained on APEmille at Zeuthen.
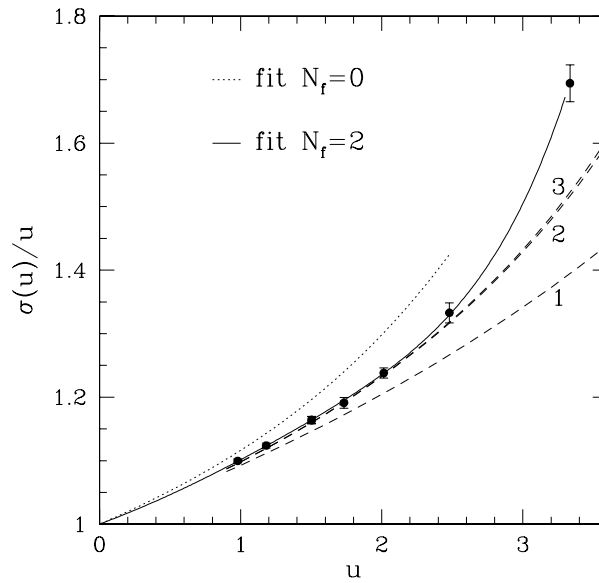

Figure 4: Step scaling function for $N_f = 2$ and $N_f = 0$ for comparison. Dashed lines are perturbative results from integrations with the one-loop and, hardly distinguishable, with the two- and three-loop β-function.

fit for $\sigma(u)$ gave only negligible changes. In this way we find the numbers in table 3. In the columns labelled by $L/a = 4$ we have replaced our continuum

	$\bar{g}^2(L_{\max}) = 3.3$			$\bar{g}^2(L'_{\max}) = 5$	
n	continuum	$L/a = 4$	n	continuum	$L/a = 4$
5	1.84(4)	1.80	6	1.24(5)	1.19
6	1.86(5)	1.78	7	1.26(5)	1.17
7	1.88(6)	1.76	8	1.28(6)	1.15

Table 3: Values estimated for $-\ln(\Lambda L_{\max})$ for two examples of $L_{\max}$.

estimates $\sigma(u)$ by $\Sigma^{(2)}(u, 1/4)$. We regard the difference between the two columns as our present systematic uncertainty[2] and quote at the moment

$$\ln(\Lambda L_{\max}) = -1.9(2) \quad [\bar{g}^2(L_{\max}) = 3.3] \tag{4.5}$$

$$\ln(\Lambda L'_{\max}) = -1.3(2) \quad [\bar{g}^2(L'_{\max}) = 5], \tag{4.6}$$

which translates into $\Lambda_{\overline{\mathrm{MS}}} L_{\max} = 0.36$ and $\Lambda_{\overline{\mathrm{MS}}} L'_{\max} = 0.66$ with about 20% total errors. A corresponding number in the quenched theory [18] for $\bar{g}^2(L_{\max}) = 3.48$ is $\ln(\Lambda L_{\max}) = -1.56(8)$ with the full continuum extrapolation and $\ln(\Lambda L_{\max}) = -1.47(2)$ under the present procedure with only statistical errors indicated here.

Finally we plot the non-perturbative evolution toward high energy for $\alpha(\mu) = \bar{g}^2(L)/4\pi$ ($\mu = 1/L$) starting from $\bar{g}^2 = 5$ in Fig. 5. Statistical errors and the difference between evolving with $\sigma(u)$ and $\Sigma^{(2)}(u, 1/4)$ are smaller than the symbol size. The overall scale error implied by the uncertainty in the start-value in eq. (4.6), which corresponds to a rigid horizontal shift of all data points, is not shown here. In comparing the non-perturbative results with the perturbative curves we emphasize that the important point to appreciate is that at high energies the expected perturbative behaviour for our coupling has been *shown* to set in. On the other hand the fact that the perturbative curves also describe the data quite well to rather low energies refers to a property of our particular observable and is definitely not to be interpreted as a reflection of some universal property of QCD couplings.

If, instead of evolving non-perturbatively, we had used three-loop perturbation theory (eq. (3.3) with $n = 0$) directly at the largest couplings $\bar{g}^2 = 3.3 \leftrightarrow \alpha = 0.26$ or $\bar{g}^2 = 5 \leftrightarrow \alpha = 0.40$, then we would have overestimated $\Lambda L_{\max}$ by 12% and 23% respectively. This in turn translates into

---

[2]A somewhat smaller value would be obtained if we took the magnitude of our perturbative improvement for lattice artefacts, $\Sigma^{(2)}(u, 1/5) - \Sigma(u, 1/5)$, as an estimate of the systematic error.
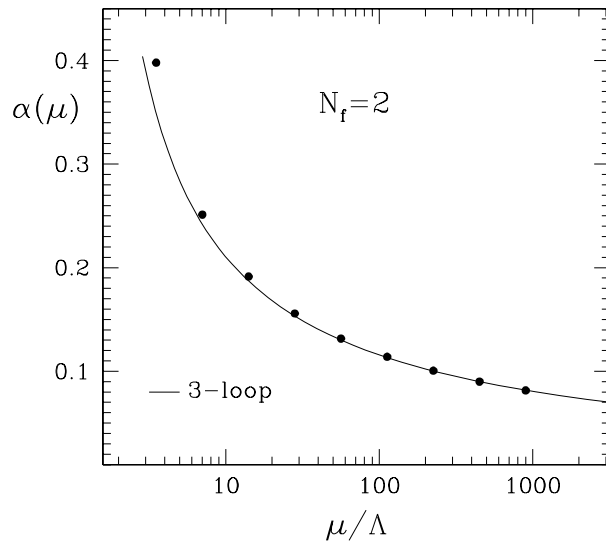
Figure 5: Evolution of $\alpha = \bar{g}^2/4\pi$ for the Schrödinger functional coupling.

errors of 2% and 5% for α in the range where its value is close to 0.12 corresponding to the physical value of $\alpha_{\overline{\text{MS}}}$ at M_{Z}. [3]

5 Conclusions

Our results demonstrate that with the generation of parallel computers being installed now a computation of $\Lambda_{\overline{\text{MS}}}$ including two massless flavours is becoming feasible with the ALPHA techniques. This includes − as in the quenched case − the possibility to probe and reduce systematic errors and, in particular, lattice spacing effects. Due to the high cost of the simulations, it is mandatory to smoothen the continuum limit as far as possible. We have therefore spent a significant effort on accompanying perturbative calculations. As observed earlier in the pure SU(2) gauge theory [20], we found that lattice artefacts of several quantities constructed in the Schrödinger functional are described quite well by perturbation theory (see Figs. 1,2). This encourages us to trust in perturbation theory to remove the lattice artefacts to a significant extent and this procedure is supported in the pure gauge theory in Fig. 3. As an estimate of the remaining systematic errors we use the difference of our results on

---

[3] For the estimate in the quenched approximation mentioned above the analogous error is smaller, since there the 3-loop β-function happens to be closer to the non-perturbative rate of evolution over the relevant range.

10

the finer lattices to those on the coarsest one. Comparing with the quenched theory, where a robust continuum extrapolation could be carried out [9,18], this error appears safe but also not over-pessimistic. Nevertheless our results still need to be corroborated by simulations closer to the continuum limit. We are in the process of simulating up to $L/a = 16$ to both reduce our errors for $\Lambda L_{\max}$ and to put them on even firmer grounds, which will however still take some time.

Already now we have clearly observed the small N_{f}-dependence of our discrete version of the β function (Fig. 4). For weak couplings its magnitude is accurately predicted by perturbation theory, while for our largest coupling ($\alpha \sim 0.25$) it overestimates the effect significantly. In particular, the use of perturbation theory for couplings up to $\alpha \sim 0.4$ in estimating Λ, would lead to a significant error already at our present level of accuracy. Moreover, this error could hardly be quantified within the framework of perturbation theory, which appears rather well behaved when looked at in isolation.

Our low energy scale still has to be gauged by an experimentally observable quantity, probably by computing $L_{\max}F_\pi$. Also the extension to $N_{\mathrm{f}} = 2$ of the non-perturbative renormalization of quark masses along the lines of ref. [18] is within reach, once the scale dependence of α is known. In the more distant future we would like to include the influence of further flavours and their masses on the evolution of the coupling.

References

[1] D. E. Groom *et al.* [Particle Data Group Collaboration], Eur. Phys. J. C **15** (2000) 1.

[2] C. T. Davies, K. Hornbostel, G. P. Lepage, P. McCallum, J. Shigemitsu and J. H. Sloan, Phys. Rev. D **56**, 2755 (1997) [hep-lat/9703010].

[3] A. Spitz *et al.* [SESAM Collaboration], Phys. Rev. D **60**, 074502 (1999) [hep-lat/9906009].

[4] A. X. El-Khadra, G. Hockney, A. S. Kronfeld and P. B. Mackenzie, Phys. Rev. Lett. **69**, 729 (1992); A. X. El-Khadra, hep-ph/9608220.

[5] R. Sommer, hep-ph/9711243.

[6] M. Lüscher, Lectures given at Les Houches Summer School 1997, hep-lat/9802029.

[7] M. Lüscher, R. Narayanan, P. Weisz and U. Wolff, Nucl. Phys. B **384**, 168 (1992) [hep-lat/9207009].

[8] S. Sint and R. Sommer, Nucl. Phys. B **465**, 71 (1996) [hep-lat/9508012].

[9] M. Lüscher, R. Sommer, P. Weisz and U. Wolff, Nucl. Phys. **B413**, 481 (1994) [hep-lat/9309005].

[10] M. Lüscher, S. Sint, R. Sommer and P. Weisz, Nucl. Phys. B **478**, 365 (1996) [hep-lat/9605038].

[11] B. Sheikholeslami and R. Wohlert, Nucl. Phys. B **259**, 572 (1985).

[12] K. Jansen and R. Sommer [ALPHA collaboration], Nucl. Phys. **B530**, 185 (1998) [hep-lat/9803017].

[13] M. Lüscher and P. Weisz, Nucl. Phys. B **479**, 429 (1996) [hep-lat/9606016].

[14] A. Bode, P. Weisz and U. Wolff [ALPHA collaboration], Nucl. Phys. B **576**, 517 (2000) [Erratum-ibid. B **600**, 453 (2001)] [2nd Erratum-ibid, to appear (2001)] [hep-lat/9911018v3].

[15] C. Christou, A. Feo, H. Panagopoulos and E. Vicari, Nucl. Phys. B **525**, 387 (1998) [Erratum-ibid, to appear (2001)] [hep-lat/9801007v2].

[16] A. Bode and H. Panagopoulos, in preparation.

[17] M. Lüscher, S. Sint, R. Sommer, P. Weisz and U. Wolff, Nucl. Phys. **B491**, 323 (1997) [hep-lat/9609035].

[18] S. Capitani, M. Lüscher, R. Sommer and H. Wittig [ALPHA Collaboration], Nucl. Phys. B **544**, 669 (1999) [hep-lat/9810063].

[19] B. Gehrmann, J. Rolf, S. Kurth and U. Wolff [ALPHA Collaboration], in preparation

[20] G. de Divitiis *et al.* [Alpha Collaboration], Nucl. Phys. B **437**, 447 (1995) [hep-lat/9411017].

[21] R. Frezzotti, M. Hasenbusch, U. Wolff, J. Heitger and K. Jansen [ALPHA Collaboration], hep-lat/0009027.